




**Multiparameter quantum estimation under dephasing noise**Le Bin Ho <sup>1,\*</sup>, Hideaki Hakoshima,<sup>2</sup> Yuichiro Matsuzaki,<sup>2</sup> Masayuki Matsuzaki <sup>3</sup>, and Yasushi Kondo <sup>1,4</sup><sup>1</sup>*Department of Physics, Kindai University, Higashi-Osaka, 577-8502, Japan*<sup>2</sup>*Device Technology Research Institute, National Institute of Advanced Industrial Science and Technology (AIST), 1-1-1, Umezono, Tsukuba, Ibaraki 305-8568, Japan*<sup>3</sup>*Department of Physics, Fukuoka University of Education, Munakata, Fukuoka 811-4192, Japan*<sup>4</sup>*Interdisciplinary Graduate School of Science and Engineering, Kindai University, Higashi-Osaka, 577-8502, Japan*

(Received 31 March 2020; accepted 14 July 2020; published 4 August 2020)

The simultaneous quantum estimation of multiple parameters has recently become an essential aspect of quantum metrology. Although the ultimate sensitivity of a multiparameter quantum estimation in a noiseless environment can overcome the standard quantum limit that every classical sensor is bounded by, it is unclear whether a quantum sensor has an advantage over a classical sensor under a realistic level of noise. In this study, we present the framework of a simultaneous estimation of multiple parameters using quantum sensors under a specific noisy environment. Three components of an external magnetic field are estimated, and we consider the dephasing noise. We show that there is an optimal sensing time in a time-inhomogeneous noisy environment and that its sensitivity can overcome the standard quantum limit.

DOI: [10.1103/PhysRevA.102.022602](https://doi.org/10.1103/PhysRevA.102.022602)**I. INTRODUCTION**

Quantum estimation theory is a mathematical framework behind quantum metrology and is important for scientific studies and technological applications. Some of its required tasks are minimizing the uncertainty of an estimation and attaining an ultimate bound imposed by the fundamental laws of quantum mechanics.

Both theoretical and experimental studies have been conducted on single-parameter estimations [1–10]. One of the practical applications of a single-parameter estimation is measuring an external field such as a magnetic or an electric field. When the resonance frequency of a solid-state qubit is shifted by an external field, we can use a superposition state of the qubit to estimate the amplitude of the external fields based on a Ramsey-type measurement. With the use of  $N$  individual qubits, we can decrease the uncertainty of the estimation by  $\delta\phi = O(N^{-\frac{1}{2}})$ , which is called the standard quantum limit (SQL). Here,  $\phi$  is a single parameter to be estimated. Moreover, by exploiting the entanglement among these  $N$  qubits, we can in principle obtain  $\delta\phi = O(N^{-1})$  in noiseless environments. This type of scaling is called the Heisenberg limit (HL) [1,5,6].

However, because an entangled state is fragile against decoherence, whether the entanglement is useful to decrease the uncertainty of the estimation in a noisy environment is not trivial. The effect of noise in single-parameter estimations has been theoretically [2,10,11] and experimentally [7,12–15] discussed. The most important noise in a solid-state qubit is a dephasing noise. It is well known that the SQL cannot be overcome in a time-homogeneous noisy environment [16]

even with the use of an entangled sensor [2]. Recent studies have shown that, if the noise is time-inhomogeneous, the scaling of  $\delta\phi = O(N^{-3/4})$  can be obtained by using entangled sensors for single-parameter estimations, and thus it overcomes the SQL [7,11,17,18]. The crucial feature of the time-inhomogeneous noise is showing a quadratic behavior as a function of time at the initial decay, which is called the Zeno regime. When the interaction time between an entangled sensor and a target field is on the order of this Zeno regime, the sensitivity of the sensor can be quantum-mechanically enhanced [11,17–19]. For an estimation of the amplitude of the field,  $\delta\phi = O(N^{-3/4})$  is considered to be the ultimate scaling under the effect of time-inhomogeneous noise [19,20].

By contrast, multiparameter estimations have received significant attention [21,22]. For example, estimations have been made of the phase and phase diffusion (loss) [23–26], phase-space displacements [27,28], multiple phases [22,29,30], damping and temperature [31], waveforms [32], and operators [33,34]. One of the practical applications of a multiparameter estimation is to measure the vector magnetic fields caused by biomaterials or a current in a circuit. These measurements are particularly important for medical and materials sciences, as discussed and demonstrated in Refs. [35,36].

In this study, we numerically investigate a multiparameter estimation under the influence of dephasing noise. In particular, we consider the estimation of three components of a target field  $\phi$  by using an entangled sensor in a noisy environment. In addition, we study the performance of an entangled sensor for both time-homogeneous and time-inhomogeneous dephasing noise [16]. Although numerical calculations of noisy quantum systems with many qubits are difficult because the size of the density matrix grows exponentially as the number of qubits increases, recent studies have shown that a calculation is tractable when the qubits are identical [37–39]. Note that such a restriction does not compromise the optimality [40,41]. We adopt this technique and investigate how the uncertainty scales

\*Present address: Research Institute of Electrical Communication, Tohoku University, Sendai 980-8577, Japan; [binho@riec.tohoku.ac.jp](mailto:binho@riec.tohoku.ac.jp).

as a function of the number of the qubits. Under the effect of time-inhomogeneous dephasing noise, we obtain the scaling  $\delta\phi = O(N^{-3/4})$ , which is the same as that of the ultimate scaling for a single-parameter estimation under dephasing noise. This implies that we can overcome the SQL for a multiparameter estimation. Our analysis will provide a further understanding of quantum metrology.

The rest of this paper is organized as follows: Section II introduces our measurement framework for estimating multiple parameters simultaneously. The numerical results are presented in Sec. III. Finally, we summarize our approach in Sec. IV.

## II. MULTIPARAMETER ESTIMATION FRAMEWORK

### A. Dynamics of a sensor with $N$ identical spins

We consider a sensor consisting of an ensemble of  $N$  identical two-level systems. The two-level system at the  $n$ th site can be characterized by the Pauli operators as  $J_\alpha^{(n)} = \frac{1}{2}\sigma_\alpha^{(n)}$  for  $\alpha = \{x, y, z\}$ . The whole sensor is similarly characterized by  $J_\alpha = \sum_n J_\alpha^{(n)}$ . To be more specific, we assume that these two-level systems are one-half spins and that the field to be sensed is a three-dimensional magnetic field  $\phi = (\phi_x, \phi_y, \phi_z)$ .

The sensor dynamics without noise are governed by the Hamiltonian

$$H(\phi) = \phi_x J_x + \phi_y J_y + \phi_z J_z. \quad (1)$$

The magnetic field provides the quantization axis of each qubit. We assume a sensor experiencing noise is governed by the quantum master equation

$$\frac{d\rho_t(\phi)}{dt} = -i[H(\phi), \rho_t(\phi)] + \mathcal{L}[\rho_t(\phi)], \quad (2)$$

where  $\rho_t(\phi)$  is the density matrix of the sensor at time  $t$ . Here, we take the natural unit system, or  $\hbar = 1$ . Furthermore, we assume the following:

$$\mathcal{L}[\rho_t(\phi)] = -\gamma_t \sum_{n=1}^N [a^{(n)}, [a^{(n)}, \rho_t(\phi)]], \quad (3)$$

where  $\gamma_t$  characterizes the strength of the noise and

$$a^{(n)} = \boldsymbol{\varphi} \cdot \mathbf{J}^{(n)} = \varphi_x J_x^{(n)} + \varphi_y J_y^{(n)} + \varphi_z J_z^{(n)}, \quad (4)$$

where  $a^{(n)}$  is the operator acting on the  $n$ th spin and is normalized such that  $[a^{(n)}]^2 = \mathbf{I}$ , or  $\varphi_x^2 + \varphi_y^2 + \varphi_z^2 = 4$ .

We then consider a dephasing noise by assuming  $\phi \parallel \boldsymbol{\varphi}$  where environmental noisy fields are applied along the quantization axis of the system. A similar noise has been considered in single-parameter estimations [11,17,21]. This assumption leads to a property in which  $H(\phi)$  and  $a^{(n)}$  commute, and thus the sensor dynamics becomes tractable. Such a dephasing noise is often considered as a dominant noise for solid-state qubit systems and in a NMR.

Time-homogeneous and time-inhomogeneous noisy environments [16] can be introduced by taking the noise strength  $\gamma_t$  as

$$\gamma_t = \begin{cases} \gamma: & \text{time homogeneous} \\ \gamma^2 t: & \text{time inhomogeneous.} \end{cases} \quad (5)$$

We provide detailed calculations for the dynamics of such a sensor in Appendixes A and B.

### B. Accuracy of estimation

The accuracy of the estimation of  $\phi$  is evaluated by using its covariance matrix,  $[V(\phi)]_{\alpha,\beta} = \langle \phi_\alpha \phi_\beta \rangle - \langle \phi_\alpha \rangle \langle \phi_\beta \rangle$ . The diagonal elements  $[V(\phi)]_{\alpha,\alpha}$  are variances  $(\delta\phi_\alpha)^2$ , whereas the off-diagonal elements are correlations between different parameters. The quantum Cramér-Rao bound is a lower bound of the covariance matrix in terms of the classical Fisher information matrix (CFIM, or  $F$ ) and quantum Fisher information matrix (QFIM, or  $Q$ ), such that

$$MV(\phi) \geq [F(\phi)]^{-1} \geq [Q(\phi)]^{-1}, \quad (6)$$

where  $M$  is the number of repeated measurements within total measurement time  $T$ . The first inequality is a classical Cramér-Rao bound (CCRB), and the second is referred to as a quantum Cramér-Rao bound (QCRB). Here,  $F$  is given through  $[F(\phi)]_{\alpha\beta} = \sum_l \frac{1}{P(l|\phi)} [\partial_\alpha P(l|\phi)] [\partial_\beta P(l|\phi)]$ , where  $\{\alpha, \beta\} = \{x, y, z\}$  in this work and  $P(l|\phi) = \text{Tr}[\Pi_l \rho_t(\phi)]$  is determined by a certain set of positive-operator-valued measures (POVMs)  $\{\Pi_l\}$ . When  $\rho_t(\phi)$  can be decomposed into  $\sum_l p_l |l\rangle\langle l|$ ,  $Q$  is given by

$$[Q(\phi)]_{\alpha,\beta} = 2 \sum_{p_l+p_{l'}>0} \frac{\langle l|\partial_\alpha \rho_t(\phi)|l'\rangle \langle l'|\partial_\beta \rho_t(\phi)|l\rangle}{p_l + p_{l'}}. \quad (7)$$

Although the value of  $l$  is exponentially large ( $2^N$ ) in this study, we can reduce the calculation cost from  $2^N$  to  $N^2$  when the qubits are symmetric in terms of the permutation operations on them, as described in detail in Appendixes A and B. We calculate Eq. (7) in Appendix C. It is worth mentioning that the achievability of the QCRB with a sensor that becomes a mixed state like in this study is not trivial. Let us consider a symmetric logarithmic derivative (SLD) operator  $L_{\phi_\alpha}$  for a measurement of parameter  $\phi_\alpha$ , which is defined by the following:  $\partial_{\phi_\alpha} \rho_t(\phi) = [L_{\phi_\alpha} \rho_t(\phi) + \rho_t(\phi) L_{\phi_\alpha}]/2$ . To achieve the QCRB (see Appendix D), a weak commutativity ( $\text{Tr}[\rho_t [L_{\phi_\alpha}, L_{\phi_\beta}]] = 0 \forall \{\alpha, \beta\} \in \{1, \dots, d\}$ ) is a necessary and sufficient condition for a sensor of which state is pure [22,42]. The relationship between the weak commutativity of SLDs and the QCRB for a mixed-state sensor in the case of collective measurements was discussed in Ref. [43]. Collective measurements of the magnetic fields have not been commonly discussed and individual measurements have typically been conducted [2,10,11,17–19], including in the present study. We are afraid that the weak commutativity condition of SLDs for a mixed state sensor in order to achieve the QCRB is still an open question.

Therefore, to investigate the ultimate sensitivity bound, we calculate  $Q$ . More specifically, we analyze

$$\mathcal{I} \equiv \text{Tr}[[Q(\phi)]^{-1}]/M, \quad (8)$$

which provides the lower bound of the total variance  $|\delta\phi|^2 = |\delta\phi_x|^2 + |\delta\phi_y|^2 + |\delta\phi_z|^2 \equiv \text{Tr}[V(\phi)]$  from Eq. (6).

### III. NUMERICAL RESULTS

#### A. Simultaneous versus individual scenarios

We consider both simultaneous and individual scenarios for an estimation. For the simultaneous scenario, three components of a field will be estimated simultaneously. The initial state is set to  $\rho_{t=0} = |\psi\rangle\langle\psi|$ , where

$$|\psi\rangle = \mathcal{N}(|\text{GHZ}\rangle_x + |\text{GHZ}\rangle_y + |\text{GHZ}\rangle_z). \quad (9)$$

Here,  $\mathcal{N}$  is the normalization constant and  $|\text{GHZ}\rangle_k$  is defined as follows:

$$|\text{GHZ}\rangle_k = \frac{|\lambda_k^{\max}\rangle + |\lambda_k^{\min}\rangle}{\sqrt{2}}, \quad (10)$$

where  $|\lambda_k^{\max}\rangle$  and  $|\lambda_k^{\min}\rangle$  are the two eigenstates of  $J_k$  ( $k = x, y, z$ ) that correspond to the maximum and minimum eigenvalues  $\lambda_k^{\max}$  and  $\lambda_k^{\min}$ , respectively. If there is no noise, an entangled sensor using the state  $|\psi\rangle$  provides the Heisenberg scaling for the multiparameter estimation [22].

For the individual scenario, each component will be estimated separately after repeated  $M/3$  measurements. In this case, we use the entangled state  $|\text{GHZ}\rangle_k$  in Eq. (10) ( $k = x, y, z$ ) to measure the corresponding magnetic-field component. This scheme is a direct application of the single-parameter estimation to vector field sensing.

We call  $\mathcal{I}$  with the initial state of  $\rho_{t=0}$  as  $\mathcal{I}_{\text{sim}}$  for the simultaneous measurement scenario. For the individual scenario, we similarly define  $\mathcal{I}_{\text{ind}}$  as

$$\mathcal{I}_{\text{ind}} = \frac{1}{M/3} (\mathcal{Q}_x^{-1} + \mathcal{Q}_y^{-1} + \mathcal{Q}_z^{-1}), \quad (11)$$

where  $\mathcal{Q}_k = [\mathcal{Q}(\phi)]_{k,k}$  ( $k = x, y, z$ ) is obtained by setting  $|\text{GHZ}\rangle_k$  as the initial state.

We emphasize that our framework here differs from that in Ref. [22], in which a noiseless case is considered, whereas we extend its calculation technique to include a sensor under a noisy environment.

#### B. Total variance under dephasing noise

We investigate the performance of the entangled sensor introduced in Sec. III A for a multiparameter estimation under the effect of dephasing noise. We examine the case of  $\phi = (2/\sqrt{3}, 2/\sqrt{3}, 2/\sqrt{3})$  in Eq. (4) and  $\phi = (0.01, 0.01, 0.01)$  in Eq. (1). Here, we assume, as is usually the case, that the necessary times for the initial-state preparation and readout are negligibly small. We fix the total time to  $T = 100$  and investigate the time-homogeneous and time-inhomogeneous noise cases.

Figure 1 shows  $\mathcal{I}_{\text{sim}}$  as a function of the measurement time  $t$  for  $N = 20$ . Note that we are allowed to measure for  $T$  and thus  $M = T/t$ . We investigate the cases  $\gamma = 0, 0.05$ , and  $0.1$ . In the absence of noise ( $\gamma = 0$ ), the longer  $t$  always gives the better measurements. When noise is present ( $\gamma \neq 0$ ), we found the minimum of  $\mathcal{I}_{\text{sim}}$  occurs as a function of  $t$ . In addition, the optimal measurement time  $t^{\text{opt}}$  is a function of  $N$ .  $t^{\text{opt}}$  for a time-homogeneous noise is shorter than  $t^{\text{opt}}$  for a time-inhomogeneous noise.

We investigate  $t_*^{\text{opt}}$  as a function of  $N$  for both the simultaneous ( $* = \text{sim}$ ) and individual ( $* = \text{ind}$ ) scenarios in both

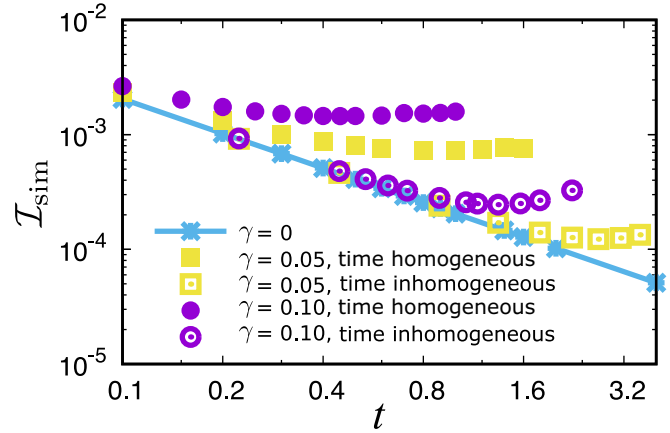


FIG. 1.  $\mathcal{I}_{\text{sim}}$  as a function of measurement time  $t$  at  $T = 100$  and  $N = 20$ . The cases at  $\gamma = 0.1$  and  $0.05$  in both time-homogeneous and time-inhomogeneous dephasing noisy environments are shown. In addition, the values of  $\mathcal{I}_{\text{sim}}$  at  $\gamma = 0$  are plotted for comparison. Note that  $M = T/t$ .

cases of time-homogeneous and time-inhomogeneous noise. Figure 2 shows that  $1/t_*^{\text{opt}}$  is proportional to  $N$  ( $\sqrt{N}$ ) in the time-homogeneous (time-inhomogeneous) case at  $N \geq 10$ , as expected [2,17]. We also found, however, that  $t_*^{\text{opt}}$  behaves differently at  $N < 10$  in both the time-homogeneous and time-inhomogeneous cases. We suspect that  $N < 10$  is too small to observe the expected dependencies. We define the minimum of  $\mathcal{I}_*$  as  $\mathcal{I}_*^{\min}$ , and  $t_*$ , which gives  $\mathcal{I}_*^{\min}$ , is defined as  $t_*^{\text{opt}}$ . These observations are consistent with the  $N$  dependence of  $\mathcal{I}_*^{\min}$ , as shown in Fig. 3.

Figure 3 shows  $\mathcal{I}_*^{\min}$  ( $* = \text{sim}$  or  $\text{ind}$ ) for  $\gamma = 0.05$  at  $t = t_*^{\text{opt}}$ , as a function of  $N$ . We observe the following for a time-homogeneous case: (i)  $\mathcal{I}_*^{\min}$  becomes proportional to  $N^{-1}$  at  $N \geq 10$  or has the same dependence as the SQL, and thus the entangled sensor has no benefit in terms of the  $N$  scaling, and (ii)  $\mathcal{I}_{\text{ind}}^{\min} > \mathcal{I}_{\text{sim}}^{\min}$  at the same  $N$ , which implies

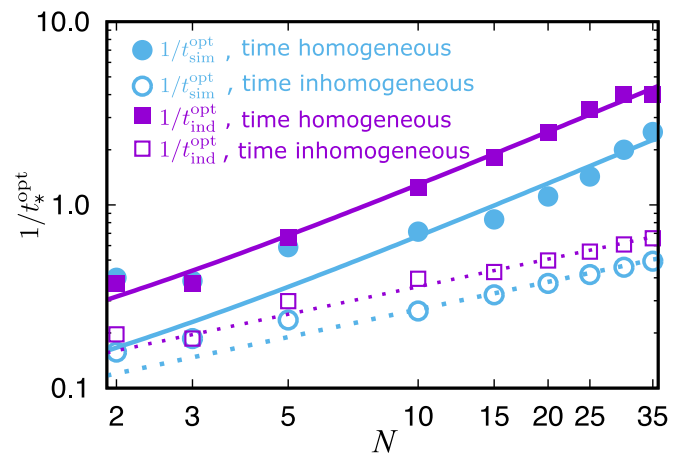


FIG. 2.  $1/t_*^{\text{opt}}$  as a function of  $N$  for two cases of time-homogeneous and time-inhomogeneous dephasing noisy environments. In addition,  $* = \text{sim}$  or  $\text{ind}$ . The dotted lines show  $\sqrt{N}$  dependence, and the solid lines indicate  $N$  dependence. We then fit the data for  $N \geq 10$ .

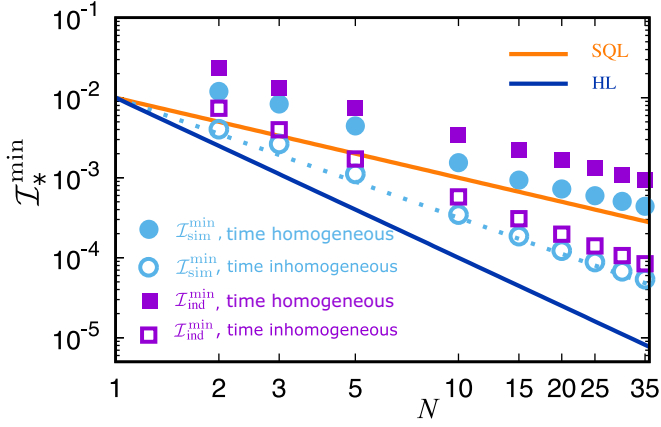


FIG. 3.  $\mathcal{I}_*^{\min}$  as a function of  $N$  in the time homogeneous and time inhomogeneous dephasing noisy environments when  $\gamma = 0.05$ . To show the SQL and HL dependencies,  $1/TN$  (orange line, SQL) and  $1/TN^2$  (blue line, HL) are plotted. The line  $1/TN^{1.5}$  is also plotted (cyan dotted line).

that a simultaneous measurement is beneficial. Such behavior is consistent with the case of a single-parameter estimation in which entangled sensors cannot overcome the SQL under the effect of the time-homogeneous dephasing noise [2].

By contrast, we observe the following for the time-inhomogeneous-noise case: (i)  $\mathcal{I}_*^{\min}$  is proportional to  $N^{-1.5}$  at  $N \geq 10$ , and thus the entangled sensor is beneficial in terms of the  $N$  scaling, and (ii)  $\mathcal{I}_{\text{ind}}^{\min} > \mathcal{I}_{\text{sim}}^{\min}$  (although this difference is small) at the same  $N$ , which implies that the simultaneous measurement is beneficial. Observation (i) ( $N^{-1.5}$  dependence) is a well-known scaling for time-inhomogeneous dephasing for a single-parameter estimation [11,17]. Observation (ii) was reported for a noiseless case [22]. In the present study, however, we show a reduction in the uncertainty of the noisy cases.

#### IV. CONCLUSION

In conclusion, we analyzed the simultaneous estimation of multiple parameters by using an entangled sensor in both time-homogeneous and time-inhomogeneous dephasing noisy environments and found that an entangled sensor is beneficial in the latter, but not in the former.

Three components of a magnetic field are the multiple parameters, which are sensed by using an ensemble of  $N$  identical one-half spins that are entangled with each other. By considering the symmetry in the permutation operations on these spins, the calculation cost is drastically reduced and becomes tractable. The entangled sensor is exposed to target fields under the effect of a dephasing noise. We numerically calculate the quantum Fisher information matrix and investigate the lower bound of the total variance. When a dephasing noise is present, it always prevents us from achieving the Heisenberg limit. However, we found that our entangled sensor can overcome the standard quantum limit in a time-inhomogeneous dephasing noisy environment but not in a time-homogeneous one.

#### ACKNOWLEDGMENTS

This work was supported by CREST (JPMJCR1774), JST, and by the Leading Initiative for Excellent Young Researchers MEXT Japan, MEXT KAKENHI (Grant No. 15H05870), and JST presto (Grant No. JPMJPR1919) Japan. L.B.H. is grateful to Nathan Shammah for the useful discussions on QuTiP.

#### APPENDIX A. PERMUTATION SYMMETRIC SENSOR

We consider a sensor consisting of  $N$  identical particles where the permutation symmetry is taken as follows [39,44,45]: The joint Hilbert space of the sensor is  $\mathcal{H}_N = \mathcal{H}^{(1)} \otimes \dots \otimes \mathcal{H}^{(N)}$  with  $\dim(\mathcal{H}_N) = 2^N$ . Any quantum state of the sensor can be given as follows:

$$|\psi\rangle = \sum_{m_1, m_2, \dots, m_N} c_{m_1, m_2, \dots, m_N} |m_1, m_2, \dots, m_N\rangle, \quad (\text{A1})$$

where the product basis  $|m_1, m_2, \dots, m_N\rangle = |m_1\rangle \otimes |m_2\rangle \otimes \dots \otimes |m_N\rangle$ , with  $m_n = \pm \frac{1}{2}$  is the eigenvalue of  $J_z^{(n)}$ . This basis is an eigenstate of the spin operators  $\mathbf{J}^{(n)}$  and  $J_z^{(n)}$

$$[\mathbf{J}^{(n)}]^2 |m_1, m_2, \dots, m_N\rangle = j_n(j_n + 1) |m_1, m_2, \dots, m_N\rangle, \quad (\text{A2})$$

$$J_z^{(n)} |m_1, m_2, \dots, m_N\rangle = m_n |m_1, m_2, \dots, m_N\rangle. \quad (\text{A3})$$

The above product basis can be represented by an irrep basis, which consists of the total spin eigenstates [44,45]

$$\mathbf{J}^2 |j, m, i\rangle = j(j+1) |j, m, i\rangle, \quad (\text{A4})$$

$$J_z |j, m, i\rangle = m |j, m, i\rangle, \quad (\text{A5})$$

where  $|j, m, i\rangle$  is the irrep basis, and  $j \leq N/2$  is the total angular momentum,  $|m| \leq j$ . For each  $j$ , the quantum number  $i = 1, \dots, d_N^j$ , where

$$d_N^j = \frac{N!(2j+1)}{(N/2-j)!(N/2+j+1)!} \quad (\text{A6})$$

is the number of degenerate irreps for each  $j$  [46] (the number of ways to combine  $N$  particles that gets the total angular momentum  $j$ ).  $|\psi\rangle$  is now represented as  $|\psi\rangle = \sum c_{j,m,i} |j, m, i\rangle$ .

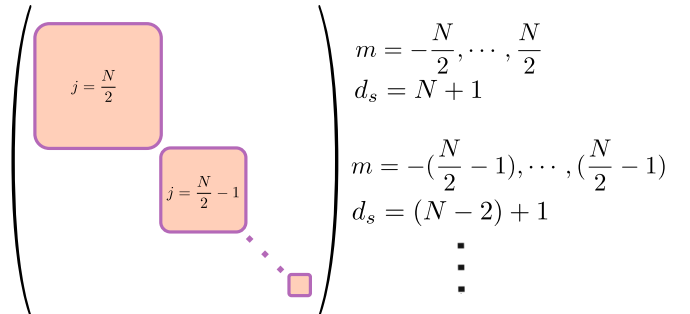


FIG. 4. Block-diagonal form of an operator in the Dicke state representation. The first block corresponds to  $j = N/2$  and its subdimension is  $d_s = N + 1$ . The same is calculated for the remaining blocks in the diagonal matrix. The off-diagonal terms are all zeros.

TABLE I. Set of  $\Gamma^{(i)}$  for  $i = 1, \dots, 27$ . Each  $\Gamma^{(i)}$  is the coefficient of  $|\dots\rangle\langle\dots|$ , respectively.

$m$	$m'$								
	$\langle j-1, m'-1  $	$\langle j-1, m'  $	$\langle j-1, m'+1  $	$\langle j, m'-1  $	$\langle j, m'  $	$\langle j, m'+1  $	$\langle j+1, m'-1  $	$\langle j+1, m'  $	$\langle j+1, m'+1  $
$ j-1, m-1\rangle$	$\Gamma^{(3)}$	$\Gamma^{(20)}$	$\Gamma^{(17)}$						
$ j-1, m\rangle$	$\Gamma^{(23)}$	$\Gamma^{(5)}$	$\Gamma^{(26)}$						
$ j-1, m+1\rangle$	$\Gamma^{(11)}$	$\Gamma^{(14)}$	$\Gamma^{(7)}$						
$ j, m-1\rangle$				$\Gamma^{(2)}$	$\Gamma^{(19)}$	$\Gamma^{(16)}$			
$ j, m\rangle$				$\Gamma^{(22)}$	$\Gamma^{(1)}$	$\Gamma^{(25)}$			
$ j, m+1\rangle$				$\Gamma^{(10)}$	$\Gamma^{(13)}$	$\Gamma^{(8)}$			
$ j+1, m-1\rangle$							$\Gamma^{(4)}$	$\Gamma^{(21)}$	$\Gamma^{(18)}$
$ j+1, m\rangle$							$\Gamma^{(24)}$	$\Gamma^{(6)}$	$\Gamma^{(27)}$
$ j+1, m+1\rangle$							$\Gamma^{(12)}$	$\Gamma^{(15)}$	$\Gamma^{(9)}$

Considering the permutation symmetry where all the degenerate irreps of each  $j$  are indistinguishable, i.e.,  $c_{j,m,i} = c_{j,m,i'} \forall i, i' \in [1, d_N^j]$ , then, the irrep basis  $|j, m, i\rangle$  can be gathered at the Dicke basis  $|j, m\rangle$  [47], where

$$|j, m\rangle = \frac{1}{\sqrt{d_N^j}} \sum_{i=1}^{d_N^j} |j, m, i\rangle. \quad (\text{A7})$$

This basis is the eigenstate of the collective pseudospin operators

$$J^2 |j, m\rangle = j(j+1) |j, m\rangle, \quad (\text{A8})$$

$$J_z |j, m\rangle = m |j, m\rangle. \quad (\text{A9})$$

Under this symmetry, the dimension now reduces to the Dicke-basis dimension  $d_D$ :

$$d_D = \begin{cases} (N+3)(N+1)/4 & \text{for odd } N \\ (N+2)^2/4 & \text{for even } N. \end{cases} \quad (\text{A10})$$

Hereinafter, we take  $\mathbf{J}$ ,  $J_\alpha$  as the collective pseudospin operators in the  $d_D$  dimension.

In the  $d_D$  dimension,  $J_\alpha$  has a structure of block matrices as shown in Fig. 4. The first block corresponds to  $j = N/2$ , and the explicit form of this block is a spin- $j$  operator  $S_\alpha$ ,  $\alpha = \{x, y, z\}$ . The construction for the others is the same. For example, for  $N = 3$ , we have

$$J_x = \begin{pmatrix} 0 & \sqrt{3}/2 & 0 & 0 & 0 & 0 \\ \sqrt{3}/2 & 0 & 2 & 0 & 0 & 0 \\ 0 & 2 & 0 & \sqrt{3}/2 & 0 & 0 \\ 0 & 0 & \sqrt{3}/2 & 0 & 0 & 0 \\ 0 & 0 & 0 & 0 & 0 & 1/2 \\ 0 & 0 & 0 & 0 & 1/2 & 0 \end{pmatrix}. \quad (\text{A11})$$

The same is applied for  $J_y$  and  $J_z$ .

## APPENDIX B. DYNAMICS OF PERMUTATION SYMMETRIC SENSOR UNDER DEPHASING NOISE

We solve Eq. (2) from the main text in  $d_D$  dimensions. Note that  $[H(\phi), a^{(n)}] = 0$ , and thus we first calculate only the Liouville term (3). The following expressions are independent of the choice of the direction of the quantization axis, which is physically determined by the target field to be measured. We rewrite this as follows:

$$\frac{\partial \rho_t}{\partial t} = 2\gamma_t \left( \sum_{n=1}^N a^{(n)} \rho_t a^{(n)} - N \rho_t \right). \quad (\text{B1})$$

We first show how to calculate the Liouvillian superoperator on the right-hand side of Eq. (B1). Using  $a^{(n)} = \varphi_x J_x^{(n)} + \varphi_y J_y^{(n)} + \varphi_z J_z^{(n)}$ , the summation term in Eq. (B1) is as follows (for short, we first keep  $\rho_t$ ):

$$\begin{aligned} \sum_{n=1}^N a^{(n)} \rho_t a^{(n)} &= \sum_{n=1}^N [\varphi_x J_x^{(n)} + \varphi_y J_y^{(n)} + \varphi_z J_z^{(n)}] \rho_t [\varphi_x J_x^{(n)} + \varphi_y J_y^{(n)} + \varphi_z J_z^{(n)}] \\ &= \sum_{n=1}^N \left[ \frac{\varphi_x}{2} (J_+^{(n)} + J_-^{(n)}) + \frac{i\varphi_y}{2} (J_-^{(n)} - J_+^{(n)}) + \varphi_z J_z^{(n)} \right] \rho_t [\dots] \\ &= \sum_{n=1}^N [\varphi_w^* J_+^{(n)} + \varphi_w J_-^{(n)} + \varphi_z J_z^{(n)}] \rho_t [\varphi_w^* J_+^{(n)} + \varphi_w J_-^{(n)} + \varphi_z J_z^{(n)}], \end{aligned} \quad (\text{B2})$$

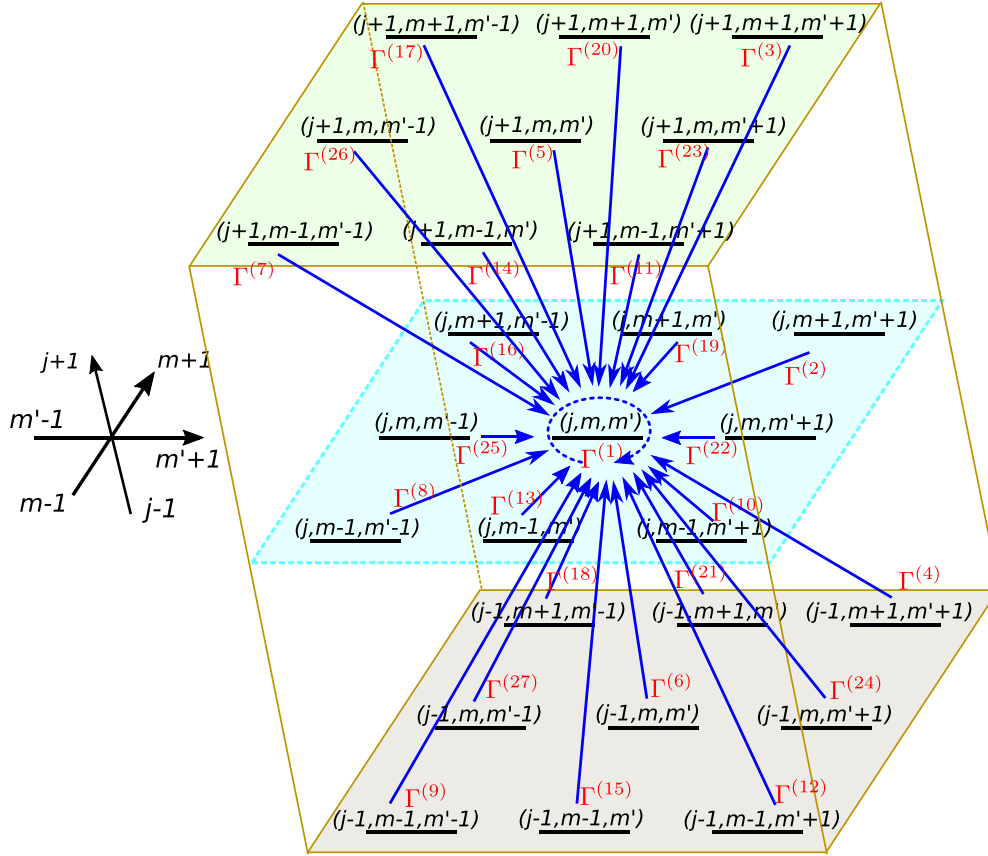


FIG. 5. Sketch of the dynamic couplings given by a Dicke state, represented in terms of the coefficients  $\Gamma^{(i)}$ . We show the action of each coefficient in the given Dicke state. All processes contribute to the coefficient  $\Gamma^{(1)}$ .

where  $J_{\pm}^{(n)} = J_x^{(n)} \pm iJ_y^{(n)}$ ,  $\varphi_w = (\varphi_x + i\varphi_y)/2$ . Finally, we have

$$\begin{aligned} \sum_{n=1}^N a^{(n)} \rho_t a^{(n)} &= \sum_{n=1}^N [(\varphi_w^*)^2 J_+^{(n)} \rho_t J_+^{(n)} + |\varphi_w|^2 J_+^{(n)} \rho_t J_-^{(n)} + \varphi_w^* \varphi_z J_+^{(n)} \rho_t J_z^{(n)} \\ &\quad + |\varphi_w|^2 J_-^{(n)} \rho_t J_+^{(n)} + (\varphi_w)^2 J_-^{(n)} \rho_t J_-^{(n)} + \varphi_w \varphi_z J_-^{(n)} \rho_t J_z^{(n)} \\ &\quad + \varphi_w^* \varphi_z J_z^{(n)} \rho_t J_+^{(n)} + \varphi_w \varphi_z J_z^{(n)} \rho_t J_-^{(n)} + \varphi_z^2 J_z^{(n)} \rho_t J_z^{(n)}]. \end{aligned} \tag{B3}$$

Here, the terms corresponding to  $J_+^{(n)} \rho_t J_-^{(n)}$ ,  $J_-^{(n)} \rho_t J_+^{(n)}$ , and  $J_z^{(n)} \rho_t J_z^{(n)}$  are local pumping, local emission, and local dephasing, respectively. Now, using  $\rho_t = \sum_{jmm'} p_{jmm'} |j, m\rangle \langle j, m'|$ , then for each  $j, m, m'$ , we have [39,44,45]

$$\sum_{n=1}^N J_k^{(n)} |j, m\rangle \langle j, m'| J_l^{(n)\dagger} = a_{kl}^N |j, m_k\rangle \langle j, m'_l| + b_{kl}^N |j-1, m_k\rangle \langle j-1, m'_l| + d_{kl}^N |j+1, m_k\rangle \langle j+1, m'_l|, \tag{B4}$$

where  $k, l = \{+, -, z\}$ ,  $m_+ = m + 1$ ,  $m_- = m - 1$ ,  $m_z = m$ , and

$$a_{kl}^N = A_k^{j,m} A_l^{j,m'} \frac{1}{2j} \left( 1 + \frac{\alpha_N^{j+1}}{d_N^j} \frac{2j+1}{j+1} \right) = A_k^{j,m} A_l^{j,m'} \frac{N/2+1}{2j(j+1)} := A_k^{j,m} A_l^{j,m'} \Lambda_a, \tag{B5}$$

$$b_{kl}^N = B_k^{j,m} B_l^{j,m'} \frac{\alpha_N^j}{2j d_N^j} = B_k^{j,m} B_l^{j,m'} \frac{N/2+j+1}{2j(2j+1)} := B_k^{j,m} B_l^{j,m'} \Lambda_b, \tag{B6}$$

$$d_{kl}^N = D_k^{j,m} D_l^{j,m'} \frac{\alpha_N^{j+1}}{2(j+1)d_N^j} = D_k^{j,m} D_l^{j,m'} \frac{N/2-j}{2(j+1)(2j+1)} := D_k^{j,m} D_l^{j,m'} \Lambda_d, \tag{B7}$$

where

$$A_{\pm}^{j,m} = \sqrt{(j \mp m)(j \pm m + 1)}, \quad A_z^{j,m} = m, \tag{B8}$$

$$B_{\pm}^{j,m} = \pm\sqrt{(j \mp m)(j \mp m - 1)}, \quad B_z^{j,m} = \sqrt{(j + m)(j - m)}, \tag{B9}$$

$$D_{\pm}^{j,m} = \mp\sqrt{(j \pm m + 1)(j \pm m + 2)}, \quad D_z^{j,m} = \sqrt{(j + m + 1)(j - m + 1)}, \tag{B10}$$

$$\Lambda_a = \frac{N/2 + 1}{2j(j + 1)}, \quad \Lambda_b = \frac{N/2 + j + 1}{2j(2j + 1)}, \quad \Lambda_d = \frac{N/2 - j}{2(j + 1)(2j + 1)}, \tag{B11}$$

and

$$\alpha_N^j = \sum_{j'=j}^{N/2} d_N^{j'} = \frac{N!}{(N/2 - j)!(N/2 + j)!}, \tag{B12}$$

with the degenerate  $d_N^j = \frac{N!(2j+1)}{(N/2-j)!(N/2+j+1)!}$ .

We calculate explicitly Eq. (B4) for each  $j, m, m'$ , where

$$\begin{aligned} \varphi_z^2 \sum_{n=1}^N J_z^{(n)} |j, m\rangle \langle j, m' | J_z^{(n)} &= \varphi_z^2 (mm' \Lambda_a |j, m\rangle \langle j, m'| &< \Gamma^{(1)} \\ &+ B_z^{j,m} B_z^{j,m'} \Lambda_b |j - 1, m\rangle \langle j - 1, m'| &< \Gamma^{(5)} \\ &+ D_z^{j,m} D_z^{j,m'} \Lambda_d |j + 1, m\rangle \langle j + 1, m'|) &< \Gamma^{(6)}. \end{aligned}$$

Here, the coefficients related to the term  $|j, m\rangle \langle j, m'|$  will be assigned ( $\leftarrow$ ) to  $\Gamma^{(1)}$  and so on:

$$\begin{aligned} |\varphi_w|^2 \sum_{n=1}^N J_-^{(n)} |j, m\rangle \langle j, m' | J_+^{(n)} &= |\varphi_w|^2 (A_-^{j,m} A_-^{j,m'} \Lambda_a |j, m - 1\rangle \langle j, m' - 1| &< \Gamma^{(2)} \\ &+ B_-^{j,m} B_-^{j,m'} \Lambda_b |j - 1, m - 1\rangle \langle j - 1, m' - 1| &< \Gamma^{(3)} \\ &+ D_-^{j,m} D_-^{j,m'} \Lambda_d |j + 1, m - 1\rangle \langle j + 1, m' - 1|) &< \Gamma^{(4)}, \\ |\varphi_w|^2 \sum_{n=1}^N J_+^{(n)} |j, m\rangle \langle j, m' | J_-^{(n)} &= |\varphi_w|^2 (A_+^{j,m} A_+^{j,m'} \Lambda_a |j, m + 1\rangle \langle j, m' + 1| &< \Gamma^{(8)} \\ &+ B_+^{j,m} B_+^{j,m'} \Lambda_b |j - 1, m + 1\rangle \langle j - 1, m' + 1| &< \Gamma^{(7)} \\ &+ D_+^{j,m} D_+^{j,m'} \Lambda_d |j + 1, m + 1\rangle \langle j + 1, m' + 1|) &< \Gamma^{(9)} \end{aligned}$$

[note that  $J_-^{(n)}$  becomes  $J_+^{(n)\dagger}$  as in Eq. (B4)],

$$\begin{aligned} (\varphi_w^*)^2 \sum_{n=1}^N J_+^{(n)} |j, m\rangle \langle j, m' | J_+^{(n)} &= (\varphi_w^*)^2 (A_+^{j,m} A_+^{j,m'} \Lambda_a |j, m + 1\rangle \langle j, m' - 1| &< \Gamma^{(10)} \\ &+ B_+^{j,m} B_-^{j,m'} \Lambda_b |j - 1, m + 1\rangle \langle j - 1, m' - 1| &< \Gamma^{(11)} \\ &+ D_+^{j,m} D_-^{j,m'} \Lambda_d |j + 1, m + 1\rangle \langle j + 1, m' - 1|) &< \Gamma^{(12)}, \\ \varphi_w^* \varphi_z \sum_{n=1}^N J_+^{(n)} |j, m\rangle \langle j, m' | J_z^{(n)} &= \varphi_w^* \varphi_z (A_+^{j,m} m' \Lambda_a |j, m + 1\rangle \langle j, m'| &< \Gamma^{(13)} \\ &+ B_+^{j,m} B_z^{j,m'} \Lambda_b |j - 1, m + 1\rangle \langle j - 1, m'| &< \Gamma^{(14)} \\ &+ D_+^{j,m} D_z^{j,m'} \Lambda_d |j + 1, m + 1\rangle \langle j + 1, m'|) &< \Gamma^{(15)}, \\ \varphi_w^2 \sum_{n=1}^N J_-^{(n)} |j, m\rangle \langle j, m' | J_-^{(n)} &= \varphi_w^2 (A_-^{j,m} A_+^{j,m'} \Lambda_a |j, m - 1\rangle \langle j, m' + 1| &< \Gamma^{(16)} \\ &+ B_-^{j,m} B_+^{j,m'} \Lambda_b |j - 1, m - 1\rangle \langle j - 1, m' + 1| &< \Gamma^{(17)} \\ &+ D_-^{j,m} D_+^{j,m'} \Lambda_d |j + 1, m - 1\rangle \langle j + 1, m' + 1|) &< \Gamma^{(18)}, \end{aligned}$$

$$\varphi_w \varphi_z \sum_{n=1}^N J_z^{(n)} |j, m\rangle \langle j, m' | J_z^{(n)} = \varphi_w \varphi_z (A_-^{j,m} m' \Lambda_a |j, m-1\rangle \langle j, m'| \quad \leftarrow \Gamma^{(19)}$$

$$+ B_-^{j,m} B_z^{j,m'} \Lambda_b |j-1, m-1\rangle \langle j-1, m'| \quad \leftarrow \Gamma^{(20)}$$

$$+ D_-^{j,m} D_z^{j,m'} \Lambda_d |j+1, m-1\rangle \langle j+1, m'| \quad \leftarrow \Gamma^{(21)},$$

$$\varphi_w^* \varphi_z \sum_{n=1}^N J_z^{(n)} |j, m\rangle \langle j, m' | J_+^{(n)} = \varphi_w^* \varphi_z (mA_-^{j,m} \Lambda_a |j, m\rangle \langle j, m'-1| \quad \leftarrow \Gamma^{(22)}$$

$$+ B_z^{j,m} B_-^{j,m'} \Lambda_b |j-1, m\rangle \langle j-1, m'-1| \quad \leftarrow \Gamma^{(23)}$$

$$+ D_z^{j,m} D_-^{j,m'} \Lambda_d |j+1, m\rangle \langle j+1, m'-1| \quad \leftarrow \Gamma^{(24)},$$

$$\varphi_w \varphi_z \sum_{n=1}^N J_z^{(n)} |j, m\rangle \langle j, m' | J_-^{(n)} = \varphi_w \varphi_z (mA_+^{j,m} \Lambda_a |j, m\rangle \langle j, m'+1| \quad \leftarrow \Gamma^{(25)}$$

$$+ B_z^{j,m} B_+^{j,m'} \Lambda_b |j-1, m\rangle \langle j-1, m'+1| \quad \leftarrow \Gamma^{(26)}$$

$$+ D_z^{j,m} D_+^{j,m'} \Lambda_d |j+1, m\rangle \langle j+1, m'+1| \quad \leftarrow \Gamma^{(27)}.$$

We collect all coefficients corresponding to each  $|\cdot\rangle\langle\cdot|$  and assign as  $\Gamma^{(i)}$ , where  $i = 1, \dots, 27$  as shown in Table I and Fig. 5.

Explicitly, we have the following:

$$\begin{aligned} \Gamma^{(1)} &= 2\gamma_t (\varphi_z^2 m m' \Lambda_a - N), & \Gamma^{(10)} &= 2\gamma_t (\varphi_w^*)^2 A_+^{j,m} A_-^{j,m'} \Lambda_a, & \Gamma^{(19)} &= 2\gamma_t \varphi_w \varphi_z A_-^{j,m} m' \Lambda_a, \\ \Gamma^{(2)} &= 2\gamma_t |\varphi_w|^2 A_-^{j,m} A_-^{j,m'} \Lambda_a, & \Gamma^{(11)} &= 2\gamma_t (\varphi_w^*)^2 B_+^{j,m} B_-^{j,m'} \Lambda_b, & \Gamma^{(20)} &= 2\gamma_t \varphi_w \varphi_z B_-^{j,m} B_z^{j,m'} \Lambda_b, \\ \Gamma^{(3)} &= 2\gamma_t |\varphi_w|^2 B_-^{j,m} B_-^{j,m'} \Lambda_b, & \Gamma^{(12)} &= 2\gamma_t (\varphi_w^*)^2 D_+^{j,m} D_-^{j,m'} \Lambda_d, & \Gamma^{(21)} &= 2\gamma_t \varphi_w \varphi_z D_-^{j,m} D_z^{j,m'} \Lambda_d, \\ \Gamma^{(4)} &= 2\gamma_t |\varphi_w|^2 D_-^{j,m} D_-^{j,m'} \Lambda_d, & \Gamma^{(13)} &= 2\gamma_t \varphi_w^* \varphi_z A_+^{j,m} m' \Lambda_a, & \Gamma^{(22)} &= 2\gamma_t \varphi_w^* \varphi_z mA_-^{j,m'} \Lambda_a, \\ \Gamma^{(5)} &= 2\gamma_t \varphi_z^2 B_z^{j,m} B_z^{j,m'} \Lambda_b, & \Gamma^{(14)} &= 2\gamma_t \varphi_w^* \varphi_z B_+^{j,m} B_z^{j,m'} \Lambda_b, & \Gamma^{(23)} &= 2\gamma_t \varphi_w^* \varphi_z B_z^{j,m} B_-^{j,m'} \Lambda_b, \\ \Gamma^{(6)} &= 2\gamma_t \varphi_z^2 D_z^{j,m} D_z^{j,m'} \Lambda_d, & \Gamma^{(15)} &= 2\gamma_t \varphi_w^* \varphi_z D_+^{j,m} D_z^{j,m'} \Lambda_d, & \Gamma^{(24)} &= 2\gamma_t \varphi_w^* \varphi_z D_z^{j,m} D_-^{j,m'} \Lambda_d, \\ \Gamma^{(7)} &= 2\gamma_t |\varphi_w|^2 B_+^{j,m} B_+^{j,m'} \Lambda_b, & \Gamma^{(16)} &= 2\gamma_t \varphi_w^2 A_-^{j,m} A_+^{j,m'} \Lambda_a, & \Gamma^{(25)} &= 2\gamma_t \varphi_w \varphi_z mA_+^{j,m'} \Lambda_a, \\ \Gamma^{(8)} &= 2\gamma_t |\varphi_w|^2 A_+^{j,m} A_+^{j,m'} \Lambda_a, & \Gamma^{(17)} &= 2\gamma_t \varphi_w^2 B_-^{j,m} B_+^{j,m'} \Lambda_b, & \Gamma^{(26)} &= 2\gamma_t \varphi_w \varphi_z B_z^{j,m} B_+^{j,m'} \Lambda_b, \\ \Gamma^{(9)} &= 2\gamma_t |\varphi_w|^2 D_+^{j,m} D_+^{j,m'} \Lambda_d, & \Gamma^{(18)} &= 2\gamma_t \varphi_w^2 D_-^{j,m} D_+^{j,m'} \Lambda_d, & \Gamma^{(27)} &= 2\gamma_t \varphi_w \varphi_z D_z^{j,m} D_+^{j,m'} \Lambda_d \end{aligned}$$

Thus, the equation can be solved. In the numerical calculation, we have extended the permutational-invariant quantum solver (PIQS) library in QUTIP [39] by using the analysis described in this Appendix.

Finally,  $\rho_t(\boldsymbol{\phi})$  is given by the evolution  $U(\boldsymbol{\phi})\rho_t U^\dagger(\boldsymbol{\phi})$ .

### APPENDIX C. CALCULATION OF THE QUANTUM FISHER INFORMATION MATRIX

To calculate the QFIM, we need

$$\begin{aligned} \partial_k \rho_t(\boldsymbol{\phi}) &= \partial_k [U(\boldsymbol{\phi})\rho_t U^\dagger(\boldsymbol{\phi})] \\ &= \partial_k U(\boldsymbol{\phi})\rho_t U^\dagger(\boldsymbol{\phi}) + U(\boldsymbol{\phi})\rho_t \partial_k U^\dagger(\boldsymbol{\phi}). \end{aligned} \quad (C1)$$

Here,  $U(\boldsymbol{\phi}) = e^{-iH(\boldsymbol{\phi})}$ . Some calculations [48] provide

$$\begin{aligned} \partial_k U(\boldsymbol{\phi}) &= \partial_k e^{-iH(\boldsymbol{\phi})} = -i \int_0^t du e^{-i(1-u)H(\boldsymbol{\phi})} [\partial_k H(\boldsymbol{\phi})] e^{-iuH(\boldsymbol{\phi})} \\ &= -i e^{-iH(\boldsymbol{\phi})} \int_0^t du e^{iuH(\boldsymbol{\phi})} J_k e^{-iuH(\boldsymbol{\phi})}. \end{aligned} \quad (C2)$$

We introduce  $A_k$  defined as follows:

$$A_k = \int_0^t du e^{iuH(\boldsymbol{\phi})} J_k e^{-iuH(\boldsymbol{\phi})}. \quad (C3)$$

$A_k$  is a Hermitian operator [22,48,49].

We calculate the QFIM [Eq. (7) in the main text] by using  $A_k$ . To obtain the explicit form of Eq. (C3) in this study, we follow the method described in Refs. [48,49]. Therein, for  $t \ll 1$ , we obtain

$$A_k \approx t J_k. \quad (C4)$$

For general values of  $t$ , we obtain [48,49]

$$A_k = t \sum_{\{l|\lambda_l=0\}} \text{Tr}[\Gamma_l^\dagger J_k] \Gamma_l - i \sum_{\{l|\lambda_l \neq 0\}} \frac{1 - e^{-i\lambda_l t}}{\lambda_l} \text{Tr}[\Gamma_l^\dagger J_k] \Gamma_l, \quad (C5)$$

where  $\Gamma$  satisfies the eigenvalue equation:

$$\mathcal{H}(\boldsymbol{\phi})\Gamma \equiv [H(\boldsymbol{\phi}), \Gamma] = \lambda\Gamma. \quad (C6)$$

Here,  $\mathcal{H}(\boldsymbol{\phi})$  is a Hermitian superoperator of  $H(\boldsymbol{\phi})$ , which has  $d_D^2$  real eigenvalues:  $\lambda_1, \dots, \lambda_{d_D^2}$ . We denote the corresponding eigenvectors as  $\Gamma_l$ , where  $l = 1, \dots, d_D^2$ , which are orthogonal to each other.



#### APPENDIX D. ACHIEVABILITY OF THE QUANTUM CRAMÉR-RAO BOUND

We emphasize that the QCRB, in general, may be unachievable owing to the noncommutativity of the measurements for different parameters. Given a symmetric logarithmic derivative (SLD) operator  $L_{\phi_\alpha}$  for the measurement of parameter  $\phi_\alpha$ , a weak commutativity condition for achieving the QCRB is as follows:

$$\text{Tr}[\rho_t(\boldsymbol{\phi})[\hat{L}_\alpha, \hat{L}_\beta]] = 0 \quad \forall \{\alpha, \beta\} \in \{1, \dots, d\}, \quad (\text{D1})$$

where  $d$  is the number of parameters [22,42]. Otherwise, a much stronger condition of  $[\hat{L}_\alpha, \hat{L}_\beta] = 0$  is necessary [25].

The condition (D1) can be expressed by using  $A_k$  as follows [22]:

$$\text{Im}[\text{Tr}[\rho_t A_\alpha A_\beta]] = 0. \quad (\text{D2})$$

This form of the achievability condition is more tractable.

As described in the main text, collective measurements on many copies of the quantum states are needed to obtain the QCRB for mixed states [43]. Such collective measurements are not assumed for a standard setup of magnetic-field sensing, and it is not clear whether we can achieve the QCRB without collective measurements. Therefore, the achievability of the QCRB is left as future work, and we focus on calculating the ultimate sensitivity bound given by the QFIM.

- 
- [1] L. Pezzé and A. Smerzi, *Phys. Rev. Lett.* **102**, 100401 (2009).
- [2] S. F. Huelga, C. Macchiavello, T. Pellizzari, A. K. Ekert, M. B. Plenio, and J. I. Cirac, *Phys. Rev. Lett.* **79**, 3865 (1997).
- [3] D. J. Wineland, J. J. Bollinger, W. M. Itano, F. L. Moore, and D. J. Heinzen, *Phys. Rev. A* **46**, R6797 (1992).
- [4] D. J. Wineland, J. J. Bollinger, W. M. Itano, and D. J. Heinzen, *Phys. Rev. A* **50**, 67 (1994).
- [5] V. Giovannetti, S. Lloyd, and L. Maccone, *Science* **306**, 1330 (2004).
- [6] V. Giovannetti, S. Lloyd, and L. Maccone, *Phys. Rev. Lett.* **96**, 010401 (2006).
- [7] J. A. Jones, S. D. Karlen, J. Fitzsimons, A. Ardavan, S. C. Benjamin, G. A. D. Briggs, and J. J. L. Morton, *Science* **324**, 1166 (2009).
- [8] S. Simmons, J. A. Jones, S. D. Karlen, A. Ardavan, and J. J. L. Morton, *Phys. Rev. A* **82**, 022330 (2010).
- [9] S. Zaiser, T. Rendler, I. Jakobi, T. Wolf, S.-Y. Lee, S. Wagner, V. Bergholm, T. Schulte-Herbrüggen, P. Neumann, and J. Wrachtrup, *Nat. Commun.* **7**, 12279 (2016).
- [10] Y. Matsuzaki, S. Benjamin, S. Nakayama, S. Saito, and W. J. Munro, *Phys. Rev. Lett.* **120**, 140501 (2018).
- [11] Y. Matsuzaki, S. C. Benjamin, and J. Fitzsimons, *Phys. Rev. A* **84**, 012103 (2011).
- [12] J. M. Taylor, P. Cappellaro, L. Childress, L. Jiang, D. Budker, P. R. Hemmer, A. Yacoby, R. Walsworth, and M. D. Lukin, *Nat. Phys.* **4**, 810 (2008).
- [13] G. de Lange, D. Ristè, V. V. Dobrovitski, and R. Hanson, *Phys. Rev. Lett.* **106**, 080802 (2011).
- [14] L. B. Ho, Y. Matsuzaki, M. Matsuzaki, and Y. Kondo, *New J. Phys.* **21**, 093008 (2019).
- [15] L. B. Ho, Y. Matsuzaki, M. Matsuzaki, and Y. Kondo, *J. Phys. Soc. Jpn.* **89**, 054001 (2020).
- [16] A. Smirne, J. Kołodyński, S. F. Huelga, and R. Demkowicz-Dobrzański, *Phys. Rev. Lett.* **116**, 120801 (2016).
- [17] A. W. Chin, S. F. Huelga, and M. B. Plenio, *Phys. Rev. Lett.* **109**, 233601 (2012).
- [18] T. Tanaka, P. Knott, Y. Matsuzaki, S. Dooley, H. Yamaguchi, W. J. Munro, and S. Saito, *Phys. Rev. Lett.* **115**, 170801 (2015).
- [19] K. Macieszczak, *Phys. Rev. A* **92**, 010102(R) (2015).
- [20] J. F. Haase, A. Smirne, J. Kołodyński, R. Demkowicz-Dobrzański, and S. F. Huelga, *New J. Phys.* **20**, 053009 (2018).
- [21] F. Albarelli, J. F. Friel, and A. Datta, *Phys. Rev. Lett.* **123**, 200503 (2019).
- [22] T. Baumgratz and A. Datta, *Phys. Rev. Lett.* **116**, 030801 (2016).
- [23] M. D. Vidrighin, G. Donati, M. G. Genoni, X.-M. Jin, W. S. Kolthammer, M. S. Kim, A. Datta, M. Barbieri, and I. A. Walmsley, *Nat. Commun.* **5**, 3532 (2014).
- [24] M. Altorio, M. G. Genoni, M. D. Vidrighin, F. Somma, and M. Barbieri, *Phys. Rev. A* **92**, 032114 (2015).
- [25] P. J. D. Crowley, A. Datta, M. Barbieri, and I. A. Walmsley, *Phys. Rev. A* **89**, 023845 (2014).
- [26] C. N. Gagatsos, B. A. Bash, S. Guha, and A. Datta, *Phys. Rev. A* **96**, 062306 (2017).
- [27] M. G. Genoni, M. G. A. Paris, G. Adesso, H. Nha, P. L. Knight, and M. S. Kim, *Phys. Rev. A* **87**, 012107 (2013).
- [28] S. Steinlechner, J. Bauchrowitz, M. Meinders, H. Müller-Ebhardt, K. Danzmann, and R. Schnabel, *Nat. Photonics* **7**, 626 (2013).
- [29] C. Vaneph, T. Tufarelli, and G. M. Genoni, *Quantum Meas. Quantum Metrol.* **1**, 12 (2013).
- [30] P. C. Humphreys, M. Barbieri, A. Datta, and I. A. Walmsley, *Phys. Rev. Lett.* **111**, 070403 (2013).
- [31] A. Monras and F. Illuminati, *Phys. Rev. A* **83**, 012315 (2011).
- [32] D. W. Berry, M. Tsang, M. J. W. Hall, and H. M. Wiseman, *Phys. Rev. X* **5**, 031018 (2015).
- [33] A. Fujiwara, *Phys. Rev. A* **65**, 012316 (2001).
- [34] M. A. Ballester, *Phys. Rev. A* **69**, 022303 (2004).
- [35] D. Le Sage, K. Arai, D. R. Glenn, S. J. DeVience, L. M. Pham, L. Rahn-Lee, M. D. Lukin, A. Yacoby, A. Komeili, and R. L. Walsworth, *Nature (London)* **496**, 486 (2013).
- [36] A. Nowodziniski, M. Chipaux, L. Toraille, V. Jacques, J.-F. Roch, and T. Debuisschert, *Microelectron. Reliab.* **55**, 1549 (2015).
- [37] A. Shankar, J. Cooper, J. G. Bohnet, J. J. Bollinger, and M. Holland, *Phys. Rev. A* **95**, 033423 (2017).
- [38] P. Kirton and J. Keeling, *Phys. Rev. Lett.* **118**, 123602 (2017).
- [39] N. Shammah, S. Ahmed, N. Lambert, S. De Liberato, and F. Nori, *Phys. Rev. A* **98**, 063815 (2018).
- [40] F. Fröwis, M. Skotiniotis, B. Kraus, and W. Dür, *New J. Phys.* **16**, 083010 (2014).

- [41] M. Oszmaniec, R. Augusiak, C. Gogolin, J. Kołodyński, A. Acín, and M. Lewenstein, *Phys. Rev. X* **6**, 041044 (2016).
- [42] M. Szczykulska, T. Baumgratz, and A. Datta, *Adv. Phys.: X* **1**, 621 (2016).
- [43] R. Demkowicz-Dobrzanski, W. Gorecki, and M. Guta, [*J. Phys. A: Math. Theor.* (to be published)], doi: [10.1088/1751-8121/ab8ef3](https://doi.org/10.1088/1751-8121/ab8ef3)
- [44] B. A. Chase and J. M. Geremia, *Phys. Rev. A* **78**, 052101 (2008).
- [45] B. Q. Baragiola, B. A. Chase, and J. M. Geremia, *Phys. Rev. A* **81**, 032104(R) (2010).
- [46] V. V. Mihailov, *J. Phys. A: Math. Gen.* **10**, 147 (1977).
- [47] R. H. Dicke, *Phys. Rev.* **93**, 99 (1954).
- [48] R. M. Wilcox, *J. Math. Phys.* **8**, 962 (1967).
- [49] S. Pang and T. A. Brun, *Phys. Rev. A* **90**, 022117 (2014).